NeuroImage 48 (2009) 415–422

Contents lists available at ScienceDirect

NeuroImage

journal homepage: www.elsevier.com/locate/ynimg

Right frontal cortex generates reward-related theta-band oscillatory activity

Gregory J. Christie *, Matthew S. Tata

The University of Lethbridge, Canada

ARTICLE INFO

Article history:
Received 20 February 2009
Revised 28 May 2009
Accepted 29 June 2009
Available online 8 July 2009

ABSTRACT

When participants in a gambling game are given feedback as to whether they won or lost the previous bet, a series of stereotypical brain electrical responses can be observed in the electroencephalogram (EEG) and the stimulus-locked Event-Related Potential (ERP). These include the Feedback-Related Mediofrontal Negativity (FRN), a posterior P300, and a feedback-induced increase in power at the theta (4 to 8 Hz) band over frontal scalp. Although the generators of the FRN and P300 have been studied previously, little is known about the generator of feedback-induced theta. We employed a gambling game in which participants chose either high-risk/high-reward or low-risk/low-reward bets to investigate these feedback-related responses. The FRN was not modulated by the riskiness of the bet, but both P300 and feedback-induced theta were of greater amplitude following high- relative to low-risk bets. Using a bilateral multi-source Beamformer approach, we localized the induced theta-band responses following wins and losses to partially overlapping regions in the right medial frontal cortex, possibly including the Anterior Cingulate. Using a dipole-fitting approach, we found that the generators of feedback-induced theta are anatomically distinct from those of the FRN and P300.

Introduction

Humans have mechanisms to identify positive and negative outcomes of their actions and to make predictions about future outcomes. Broadly construed, these mechanisms probably serve two functions: first, to guide our current actions by keeping us engaged in beneficial behaviors and causing us to disengage from detrimental behaviors, and second, to guide learning processes that influence future behaviors. The functional neurobiology of these reward processing systems can be investigated in the laboratory using neuroimaging techniques in conjunction with gambling or guessing games that provide feedback about good or bad choices.

When a feedback stimulus indicates a win or a loss to the player in a gambling game, a stereotypical series of deflections is evoked in the Event-Related Potential (ERP). Two components have been of particular interest: the feedback-related negativity (FRN, possibly related to the feedback error-related negativity) and the feedback-related P300. The FRN is a fronto-central negative difference in the ERP following losses or negative feedback and is thought to be generated within the Anterior Cingulate (ACC) (Gehring and Willoughby, 2002). It is associated with reward-based learning (Bellebaum and Daum, 2008) and adaptive decision-making (Cohen et al., 2007). The FRN reflects more than the simple registration of "win" or "lose": its magnitude is modulated by expectancy. Small wins generate an FRN if the alternative outcome was a bigger win (Holroyd et al., 2004). There is a correlation between FRN amplitude and response switching (Yasuda et al., 2004), FRN amplitude decreases as participants improve in a learning task (Krigolson et al., 2008), and FRN-like activity can be elicited by unexpected positive feedback (Holroyd et al., 2008; Oliveira et al., 2007). There is also evidence suggesting that the evaluative properties of the FRN are affected by the motivational significance of a given task (Donkers et al., 2005; Yeung et al., 2005). Together, these results suggest that the FRN reflects reward prediction errors and thus may represent the function of a neural system mediating reinforcement learning (Holroyd et al., 2004). The feedback-related P300 is a posterior potential that has been found following feedback about wins and losses in gambling games (Yeung et al., 2005; Yeung and Sanfey, 2004) and in a learning task with a monetary reward (Bellebaum and Daum, 2008). Unlike the FRN, the P300 seems to be related to the probability or risk associated with a particular outcome and not to the valence (winning or losing) of that outcome (Yeung and Sanfey, 2004).

In addition to the feedback-evoked FRN and P300, recent investigations have identified an induced oscillatory response in the theta-band (4–8 Hz) during feedback processing (Cohen et al., 2007; Gehring and Willoughby, 2004; Marco-Pallares et al., 2008). This induced response is greater in power and phase coherence following losses relative to wins. Induced responses to wins, however, are modulated more by reward probability than are responses to losses, and are greatest in power and phase coherence when there is a low probability of winning (Cohen et al., 2007). It has been suggested that this oscillatory activity represents the functional coupling of several mediofrontal brain structures involved in feedback processing.

* Corresponding author. University of Lethbridge, Neuroscience, 4401 University Drive, Lethbridge, Alberta, Canada T1K 3M4.
E-mail address: greg.christie@uleth.ca (G.J. Christie).

1053-8119/$ – see front matter © 2009 Elsevier Inc. All rights reserved.
doi:10.1016/j.neuroimage.2009.06.076

However, the neuroanatomical generators of this induced theta-band power have yet to be identified.

Despite substantial work to investigate reward processing mechanisms in animals (see e.g. Everitt et al., 2001; Schultz, 2007), the functional anatomy of these circuits in humans remains poorly understood. Studies using functional Magnetic Resonance Imaging (fMRI) have implicated a distributed network of subcortical and frontal cortical structures mediating reward processing (Delgado et al., 2000; McClure et al., 2003; McClure et al., 2004; O'Doherty et al., 2004; O'Doherty et al., 2002; Pagnoni et al., 2002; Schonberg et al., 2007). This network includes the ventral striatum and medial orbitofrontal cortex in reward processing and the lateral orbitofrontal cortex and ACC in loss processing (Liu et al., 2007). Although the components of a frontal reward processing network have thus been identified based on metabolic activity, the electrical activity within this network has not yet been fully characterized. One study using intracranial electrodes in a neurosurgical patient found feedback-related ERP responses in the alpha band within paracingulate cortex (Oya et al., 2005). Electrical Source Imaging of the FRN (Donkers et al., 2005; Gehring and Willoughby, 2002; Holroyd et al., 2006; Holroyd et al., 2004; Marco-Pallares et al., 2008; Miltner et al., 1997; Nieuwenhuis et al., 2004a, 2004b; Yeung et al., 2005; Yeung and Sanfey, 2004) has consistently found one or more generator(s) on the anterior medial wall of the frontal lobe, possibly in ACC, suggesting that this structure contributes to reward processing. However, using a dipole analysis constrained by fMRI data, Nieuwenhuis et al. (2005) found evidence for a more distributed network involving rostral anterior cingulate, posterior cingulate, and right superior frontal gyrus.

It is unclear whether generators within ACC or elsewhere account for the feedback-induced theta-band power observed in other studies. The peak of the FRN and the peak increase in induced theta-band power are at similar latencies (approximately 250 ms post-stimulus), and both components appear to originate in right-hemisphere mediofrontal cortex (see Results section). Using a gambling paradigm, Cohen et al. (2007) observed an enhanced theta-band activity during the window of the FRN. Taken together, this suggests a functional relationship between the FRN and increases in theta-band activity. The FRN may originate due to transient phase-locking of induced oscillatory theta-band activity. Conversely, the observed increase in theta-band power may be the result of the neural activity generating the evoked FRN. To date, no study has determined the relationship, if any, between these two components. A study by Luu et al. (2003) used a dipole-fitting approach on filtered ERP data to examine feedback-evoked theta power and found possible generators in rostral ACC and in dorsal medial frontal cortex. Here we report evidence based on a beamforming approach that feedback-induced theta power is indeed generated primarily in the right mediofrontal cortex.

Our study used a gambling game similar to the Iowa Gambling Task to investigate the functional anatomy of feedback-induced neural activity. All test participants were undergraduate students who received only a fixed, non-monetary reward of 2% bonus course credit. Gambling-game experiments frequently use a variable monetary reward, and subjects are motivated by financial gain to perform well on the experimental task. Because our reward is not based on performance, our test subjects had no direct, salient incentive to care about the magnitude of the bets they placed or the feedback they received. Nevertheless, we hypothesized that measured feedback-related P300 and FRN effects would be modulated by risk and valence as reported in other literature. Subsequently, we wished to extend our data to address three unanswered questions regarding the mechanisms of feedback processing. First, what are the anatomical generators of the observed theta-band signal, and does this activity arise from within ACC? Second, is the neural activity of this theta-band generator modulated by the riskiness of the bet that led to the reward? Finally, what relationship, if any, exists between the FRN, the P300 and the increase in an induced theta-band activity? We used a three-stage process to analyze our data. First, to ensure our use of fixed reward engaged normal feedback processing, we replicated the results of previous studies with respect to FRN, P300, and oscillatory theta-band activity. Subsequently, we used the Beamformer spatial filtering technique to localize cortical sources of feedback-induced theta-band activity (Green and McDonald, 2008; Green and McDonald, in press; Gross et al., 2001; Van Veen et al., 1997), and concluded by implementing a dipole-fitting method, constrained by our Beamformer results, to identify the extent to which cortical regions associated with theta-band activity were also implicated in generating the FRN.

Materials and methods

Participants

Twenty-five undergraduate students at the University of Lethbridge participated for course credit (but not monetary reward). Of these, data from two were excluded after debriefing because they indicated they had used a card-counting strategy to try to "beat" the game. Data from four participants were excluded because of excessive eye-movement artifact (see below). Thus, data from 19 participants (12 females, mean age 22.0, two left-handed) were entered into our analysis. Participants were screened with the Canadian Problem Gambling Index (CPGI) to exclude individuals who gamble excessively and none reached exclusion criteria (the mean CPGI score was 0.9). Procedures were in accordance with the Declaration of Helsinki and were approved by the University of Lethbridge Human Subjects Review Committee; all participants gave written informed consent.

Gambling task

Participants in gambling tasks form an implicit understanding of the risks and rewards of the various choice options and adjust their selections accordingly (Bechara et al., 1994; Cavedini et al., 2002; Goudriaan et al., 2005). A computerized version of the Iowa Gambling Task (IGT) was administered prior to EEG recording so that participants gained an implicit understanding that high-risk bets were disadvantageous over long-term play. They then participated in an adaptation of the IGT suitable for the ERP technique (similar also to previous tasks used to elicit the FRN) (Gehring and Willoughby, 2002; Hewig et al., 2006; Nieuwenhuis et al., 2004a; Oya et al., 2005; Yacubian et al., 2006; Yeung et al., 2005). The paradigm consisted of a main screen with a horizontal bar at the top, which displayed the subject's current winnings or losses. Buttons at the center of the screen allowed the participant to specify either a small ($50) or large ($100) bet and to play the selected bet by clicking with a computer mouse. Upon pressing the play button, a central fixation cross appeared. A colored square then appeared after a random (uniformly distributed) duration of 500 to 1500 ms. A green square indicated a win and a red square indicated loss on the current trial. This feedback stimulus remained visible for 1000 ms and then the betting screen reappeared. Participants either won or lost the value of their wager. The win/loss schedule was pseudorandom (randomized within runs of 10 trials) with a 0.6/0.4 win/loss probability for the $50 bet and a 0.4/0.6 win/loss probability with the $100 bet. Thus there were four possible outcomes: High-Risk Win (40% chance after betting "high"), High-Risk Loss (60% chance after betting "high"), Low-Risk Win (60% chance after betting "low"), and Low-Risk Loss (40% chance after betting "low"). Participants played the game for 45 min or until 400 trials had been completed, whichever came first.

EEG recording and analysis

The electroencephalogram (EEG) was recorded from 128 sites at a 500 Hz sampling rate using Ag/AgCl electrodes in a geodesic net (Electrical Geodesics Inc., Eugene, OR, USA). Electrode placement was

recorded with a Polhemus Fast-Trak (Polhemus, Colchester, VT, USA) for later registration with the EEG dataset. Impedances were maintained below 100 kΩ. The montage was initially referenced to the vertex and then digitally re-referenced to an average reference. Data were imported into the BESA software package (Megis Software, Grafelfing, Germany) for further analysis. The record was visually inspected for bad channels and the signal from a small number of electrodes was replaced with interpolated signal (approximately five per participant; ocular, reference, and channels of interest were not interpolated). Ocular artifacts were corrected using the adaptive artifact correction algorithm (Ille et al., 2002). HEOG and VEOG threshold voltages were 150 μV and 250 μV respectively.

Analysis of evoked activity

The event-related potential (ERP) was computed by averaging the EEG in a 1000 ms window, with a 200 ms pre-stimulus baseline, time-locked to feedback presentation. Epochs with amplitude greater than 120 μV were rejected during automatic artifact scanning. Epochs were averaged within the four conditions and the waveforms interpolated into a standard 81-electrode montage in the 10–20 system to minimize electrode placement errors across participants. The data were then grand-averaged and filtered with high-pass (0.6 Hz, 6 dB/octave) and low-pass (30 Hz, 12 dB/octave) zero-phase Butterworth filters.

The FRN was identified as the largest difference between the win and loss waveforms at an approximate latency of 246 ms post-stimulus. The mean amplitude of the FRN was computed inside a window spanning approximately 50 ms on either side of this peak, from 200 to 300 ms post-stimulus. Similarly, the P300 was identified as the peak of the positive-going deflection in the waveform of each condition, identified at a latency of approximately 330 ms in all conditions. The amplitude of the P300 was measured as the mean amplitude in a window spanning 20 ms on either side of this peak, from 310 and 350 ms post-stimulus. These windows are broadly consistent with previous studies (Holroyd and Coles, 2002) and appeared to capture the important differences between different conditions. In the analysis to follow we take the FRN to be the mean difference between the peaks in this window, not the absolute amplitudes of these waves, as in the P300. For isopotential maps the difference wave was computed by subtracting High-Risk Loss from High-Risk Win waveforms and Low-Risk Loss from Low-Risk Win waveforms.

A repeated-measures ANOVA with two levels of the factor risk (high/low) and two levels of the factor valence (win/loss) was performed on the mean amplitude of the evoked activity. For the FRN the ANOVA was performed at electrode FCz between 200 and 300 ms and for the P300 the ANOVA was performed at CPz between 310 and 350 ms.

Time–frequency analysis

Time–frequency (TF) plots were calculated using BESA for each participant's four conditions within a frequency range of 4.0 to 50.0 Hz with a 2.0 Hz/25 ms sampling resolution. These values were selected to provide a maximal tradeoff in accuracy between frequency and time resolution. The Fieldtrip (F.C. Donders Centre, Nijmegen, Netherlands) toolbox for Matlab (The Mathworks, Natick, MA, USA) was used to create averaged TF plots across all participants for each of the four conditions. An ANOVA with two levels of the factor risk (high/low) and two levels of the factor valence (win/loss) was performed on the theta-band amplitude during the 150–350 ms post-stimulus interval.

A bilateral multi-source Beamformer technique (Hoechstetter et al., 2004) was used to image the intracranial signal sources of induced theta-band power subsequent to both wins and losses. Beamformer images were generated using BESA within a 150–350 ms post-stimulus interval (−200 to 0 baseline) for a signal between 4 and 8 Hz, using a four-shell ellipsoid head model and the original 128-channel montage. The beamforming approach results in four (one per condition) 3D volumetric datasets for each participant in which the parameter *Q*, a measure of signal strength in the epoch of interest relative to baseline, is computed for each voxel. These volume maps were imported into the BrainVoyager QX software package (Brain Innovation B.V., Maastricht, Netherlands). Rather than average across participants, we identified voxels that were most likely to have exhibited increased theta signal relative to baseline. For each voxel, a one-tailed *t*-test was used to compare the mean *Q* value to zero. As is commonly done in fMRI work, the resulting volume map of *t*-scores was thresholded at $p<0.001$ (uncorrected for multiple comparisons).

Dipole-fitting analysis

We tested the hypothesis that the FRN and/or the P300 might reflect a transient phase-locking of theta by considering whether our computed theta sources could account for the grand-average FRN and/or P300 ERP components in a multiple dipole model of brain electrical activity. Electrical source analysis (BESA) was applied to the 20 ms window centered on the peak of the FRN, which we have described as the difference wave between wins and losses at a given bet magnitude. A multi-source dipole-fitting solution was computed inside the BESA program for the 240–260 ms post-stimulus window. The same analysis was repeated on the 320–340 ms post-stimulus window of the P300 for the High-Risk Win and High-Risk Loss waveforms. Because of well-known spatial limitations of the dipole-fitting technique (see for e.g. Green et al., 2008) this procedure is best attempted using dipole locations constrained by a priori knowledge of the underlying functional anatomy. In this analysis our dipoles were placed at the two foci of increased theta activity obtained from our Beamformer analysis of High-Risk Wins and High-Risk Losses. Dipoles were fixed at the Talairach coordinates of the focus for High-Risk Loss (19, 33, 12) and the maximum focus for High-Risk Win (25, 17, 28). We also modeled a three-dipole solution for the same difference wave with an additional dipole placed at a second focus of theta activity in the beamformed High-Risk Win condition (31, 25, 7). Finally, to determine the extent to which the FRN and P300 components are generated by bilateral theta generators, we repeated these analyses using four- and six-dipole models, with additional dipoles mirrored into the left hemisphere at Talairach coordinates −25, 17, 28; −19, 33, 12; and −31, 25, 7. For the FRN component, a forward solution was computed for the High-Risk Losses − High-Risk Wins difference wave, and for the P300 component, forward solutions were computed using the High-Risk Win and High-Risk Loss waveforms.

Results

Behavioral results

Participants registered an average of 342 wagers (±90.2). Of these, the Low-Risk $50 bet was selected 69.7% of the time and the High-Risk $100 bet was selected 30.3% of the time (±12.6%). The absolute outcomes of the four experimental conditions were thus: 12.1% for High-Risk Wins, 18.2% for High-Risk Losses, 41.8% for Low-Risk Wins, and 27.9% for Low-Risk Losses (note that the subsequent electrophysiological results consider the smaller subset of trials that were accepted as artifact-free).

Electrophysiological results

Participants in this gambling task demonstrated both FRN (Figs. 1A, 3A) and P300 effects (Figs. 1B, 3B) consistent with previous literature. The FRN had slightly right-lateralized frontal scalp

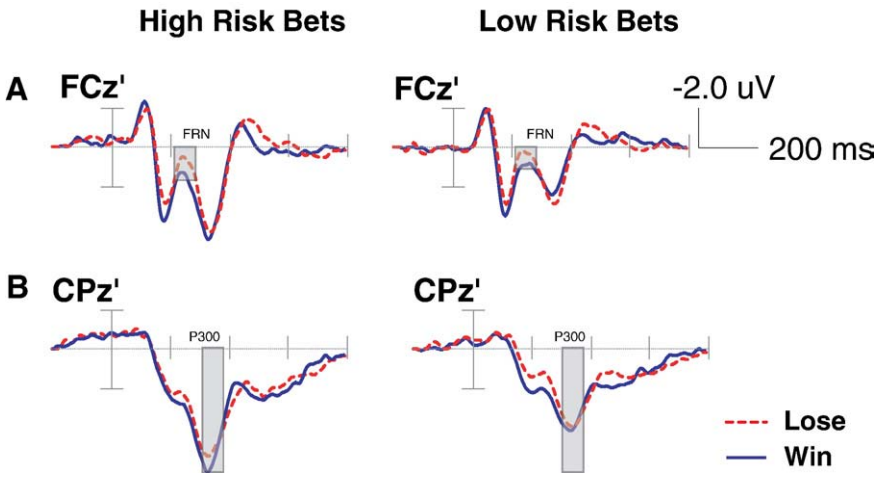

Fig. 1. Grand-averaged ERP waveforms showing FRN and P300 effects for wins and losses following feedback on high-risk/high-reward bets and low-risk/low-reward bets at selected sites. (A) The feedback-related negativity, indicated by shading, is the difference between Win and Loss waveforms at about 245 ms. (B) The P300, indicated by shading, is the positive deflection at about 330 ms.

distribution (Figs. 2A and B). Differences in P300 scalp distributions were midline and posterior (Figs. 2C and D).

We observed an FRN during the feedback window from 200 to 300 ms, as evidenced by a significant main effect of valence (win vs. loss) [$F_{1,18} = 7.135$; $p = 0.016$]. We also found a significant main effect of risk (high vs. low) [$F_{1,18} = 30.494$; $p < 0.001$], however the interaction was not significant [$F_{1,18} = 1.497$; $p = 0.237$] (Fig. 3C). Since the FRN is usually taken to be the difference between wins and losses (i.e. the effect of valence), we thus conclude that the FRN was not modulated by risk in our paradigm (non-significant interaction). To rule out deviations from expectancy we compared two outcomes with identical expected probabilities: High-Risk Wins and Low-Risk Losses (both have an EP of 40%). A post-hoc comparison was made between the mean amplitudes of the High-Risk Win and Low-Risk Loss waveforms

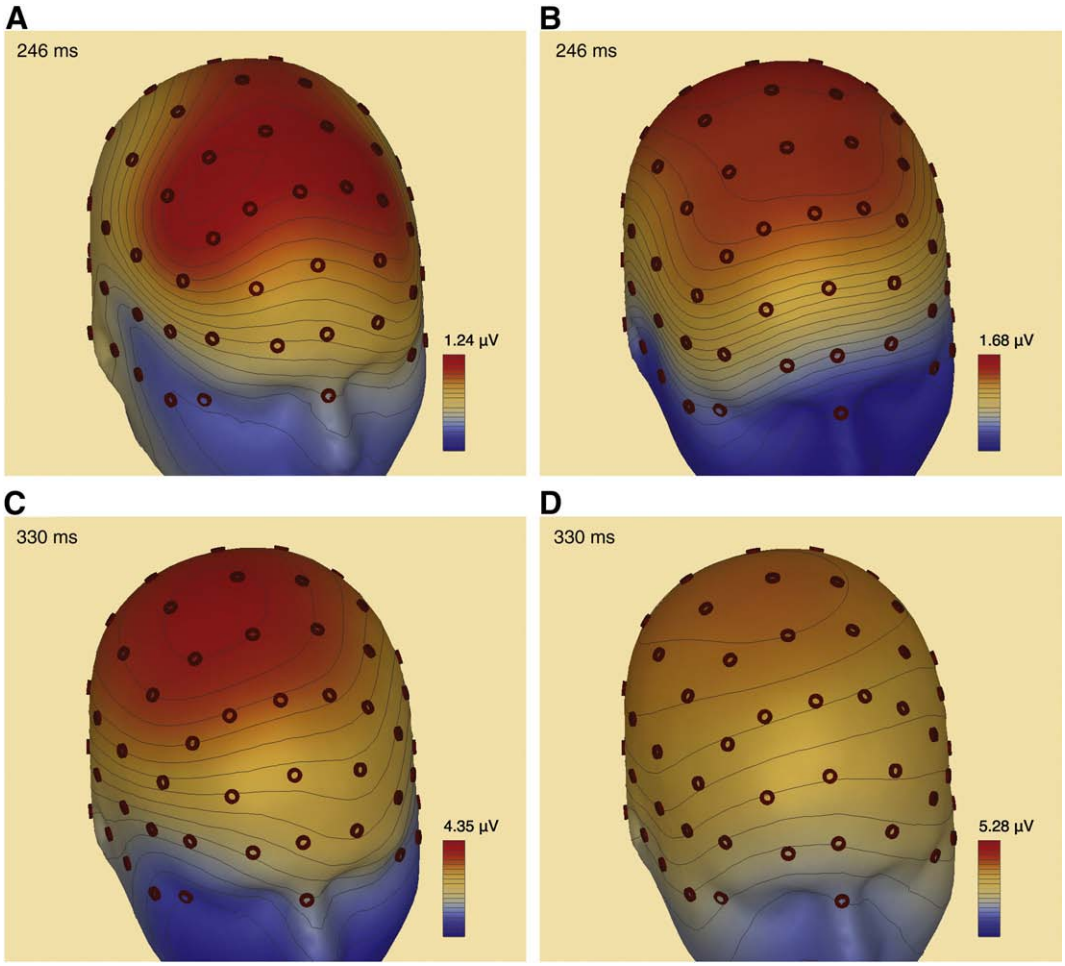

Fig. 2. Distribution of scalp voltages during feedback processing, overlaid onto an average head model. Distribution of the Win – Loss FRN following feedback on (A) high-risk/high-reward bets and (B) low-risk/low-reward bets. Scalp distribution of P300 modulation due to risk (high minus low) on (C) winning trials and (D) losing trials.

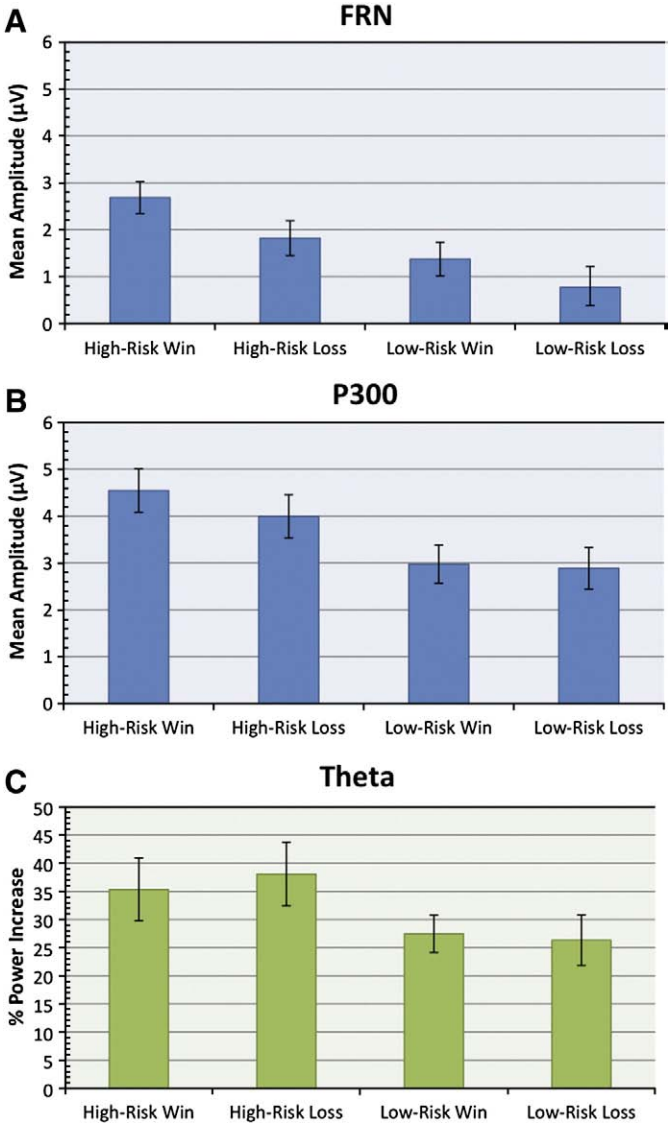

Fig. 3. Mean amplitudes (in μV) of feedback-evoked potentials (A) during the FRN window: 200–300 ms; (B) during the P300 window: 310–350 ms. (C) Power changes (in percent) in induced theta-band oscillatory window: 150–350 ms. Frequency range (theta activity): 4–8 Hz. Error bars depict standard error of the mean.

during the 200–300 ms window; the mean amplitudes of the two waveforms differed significantly [$t_{18} = 5.002$; $p < 0.001$].

During the 310 to 350 ms interval the P300 was larger in High- relative to Low-Risk bets, but its amplitude was not affected by valence. We observed a significant main effect of risk [$F_{1,18} = 28.898$; $p < 0.001$], but not of valence [$F_{1,18} = 1.701$; $p = 0.209$], and the interaction between risk and valence was only marginally significant [$F_{1,18} = 2.844$; $p = 0.109$](Fig. 4).

Feedback-induced increases in theta-band (4–8 Hz) amplitude over baseline were modulated by risk (Fig. 3) [$F_{1,18} = 10.004$; $p = 0.005$] but did not differ significantly with valence [$F_{1,18} = 0.058$; $p = 0.812$], nor was the interaction between risk and valence significant [$F_{1,18} = 0.402$; $p = 0.534$]. Beamformer analysis revealed regions of voxels significant at the $p < 0.001$ level in the High-Risk Loss and High-Risk Win conditions (Fig. 5) but were not observed in either of the Low-Risk conditions. These regions were only partially overlapping, with High-Risk Loss activity focused at Talairach coordinates 19, 33, 12, and High-Risk Win activity at two foci: 25, 17, 28 and 31, 25, 7.

The Beamformer-constrained two-dipole forward solution, with dipoles fixed at the foci of increased theta-band activity (but allowed to rotate), yielded a solution with a mean Residual Variance (RV) of 31.8% during the FRN window. The three-dipole model, with an additional dipole obtained from the High-Risk Win condition, yielded a forward solution with 30.9% RV. Mirrored into the left hemisphere, the four-dipole and six-dipole models yielded solutions with 26.0% and 24.1% RV, respectively. An analysis of the P300 component using the High-Risk Wins waveform yielded increasingly accurate forward solutions with 18.1% RV (2-dipole), 13.9% RV (3-dipole), 9.5% RV (4-dipole), and 5.4% RV (6-dipole). An analysis using the High-Risk Losses waveform yielded nearly identical forward solutions with RVs of 18.2%, 13.9%, 11.1%, and 6.0%.

Discussion

A substantial body of literature suggests that reward processing – recognizing positive and negative feedback and registering the associated probabilities of each outcome – is mediated by a network of cortical and subcortical structures (see Holroyd and Coles (2002) for review). Our study has replicated the main findings of previous work: we found significant FRN and P300 components following feedback in a gambling task. Recent investigations of induced oscillatory activity following reward feedback have revealed an induced increase in theta-band power (4–8 Hz) after feedback presentation (Cohen, 2007; Cohen et al., 2008; Luu et al., 2003; Marco-Pallares et al., 2008). We have also replicated this finding: we found a significant increase in low-frequency power following reward feedback. We tentatively ascribe the observed increase in low-frequency activity to the theta-band as this is parsimonious with other studies (Marco-Pallares et al., 2008) but we do not discount the possibility of additional signal generators in the low alpha band (8–10 Hz).

The mean amplitude of the P300 was modulated by the riskiness of the selected bet whereas the mean amplitude of the FRN was modulated by the valence of the outcome. Both the FRN and P300 responses are sensitive to stimulus probability (Cohen et al., 2007) and infrequent outcomes are known to increase the amplitude of these responses. In this study we must consider the effects of two related forms of stimulus probability: the *expected probability*, which is the implicit understanding formed by a test subject as to the likelihood of obtaining a win or a loss for a selected bet, and the *absolute probability* of a given stimulus, which is the frequency at which a stimulus was physically experienced. A recent theory suggests the FRN reflects activity of midbrain dopaminergic neurons coding for deviations from expected outcome (Holroyd and Coles, 2002) consistent with a Reinforcement Learning theory of the FRN (Krigolson et al., 2008; see also Sutton and Barto, 1998). Consequently, the size of the FRN should be larger subsequent to larger deviations from expected outcome. To rule out deviations from expectancy we compared two outcomes with identical expected probabilities: High-Risk Wins and Low-Risk Losses (both have an EP of 40%). If the FRN codes only for deviations from expected outcome we would expect to find no difference in the amplitudes of these two waveforms. Instead we observed a considerable difference between the two ERPs. These results are especially noteworthy because of our choice of reward: test participants received a fixed, non-monetary reward of bonus course credit regardless of their performance in the gambling game. Although our participants had no salient motivation to care about the bets they placed or the feedback they received, our electrophysiological data are similar to those observed in other studies on feedback processing. We interpret these data collectively to suggest that the FRN encodes relative risk in determining expected outcome, which is in turn broadly consistent with the theory that the FRN is affected by the motivational significance of events.

Theta-band activity was modulated by the riskiness of the selected wager but did not significantly differ with the valence of the outcome. The present study extends previous work by providing strong evidence that feedback-related theta power is generated by right-

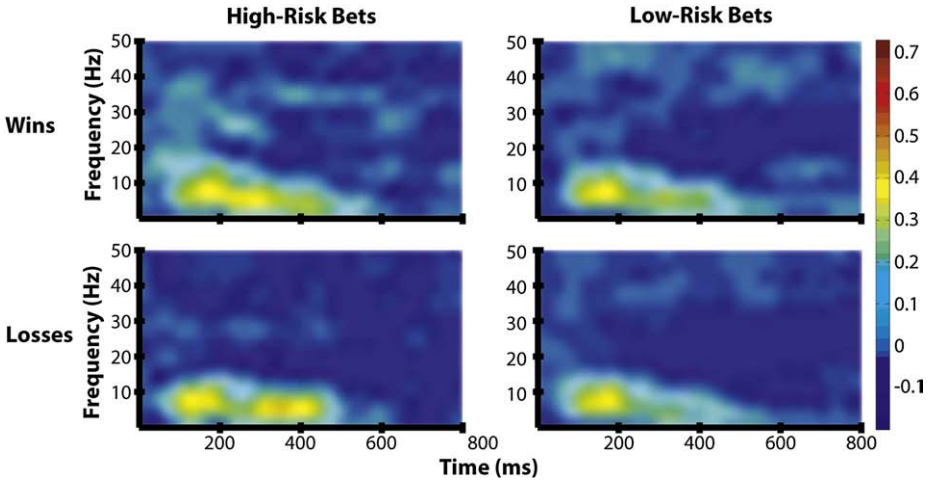

Fig. 4. Time–frequency plots showing induced theta (4–8 Hz) at FCz for each condition at a time and frequency sampling resolution of 2.0 Hz/25 ms.

hemisphere medial frontal structures. This evidence comes from a novel electrical source imaging approach, the volumetric analysis of Beamformer data, which had not yet been applied to this phenomenon. These data also support theoretical arguments that implicate the anterior cingulate cortex in monitoring feedback in cognitive tasks (Holroyd and Coles, 2002).

Of interest is the extent to which the observed increase in induced theta-band output is related to the neural processes that give rise to the FRN. To address this we used a dipole-fitting approach with several candidate models using the foci obtained from our Beamformer analysis of the High-Risk Win and High-Risk Loss conditions. Two- and three-dipole solutions yielded only partially accurate forward solutions. This inability of theta foci to account for the generators of the FRN suggests that the FRN and feedback-induced theta share only partially overlapping generators in right-hemisphere medial frontal cortex. It may be that the FRN also entails one or more frequency components outside of the theta-band that could not be accounted for by dipoles constrained to be at generators of theta oscillations. We conclude that feedback-evoked FRN represents more than a transient phase-locking of feedback-induced theta. As a general rule in dipole modeling, increasing the number of dipoles improves the accuracy of the forward solution and diminishes the residual variance, however adding two and three left-hemisphere dipoles symmetric to those in the right hemisphere improved the model's fit to the FRN only slightly. Thus, the FRN and the feedback-induced theta in our study are similar in their tendency to be right-lateralized.

A Beamformer-constrained dipole analysis of the P300 yielded solutions with greater accuracy than those of the FRN. Additionally, the accuracy of the P300 solutions increased substantially when dipoles were mirrored into the left hemisphere, suggesting the presence of bilateral generators for the P300. This indicates that the P300 component is generated bilaterally and may be more functionally and anatomically similar to the feedback-induced theta oscillation than the FRN. We believe that this is most likely the result of our operational definition of the FRN. In this analysis the FRN was identified as the difference between the evoked potentials to positive and negative feedback. The Beamformer-restrained dipole analysis thus localized electrical signals common to both positive and negative feedback. Applying this analytical technique to the feedback N200 may reveal an important difference in the relationship between induced oscillatory theta activity and the evoked electrical responses to positive and negative valence.

Theta-band oscillations within a reward processing network

Oscillations in the theta-band have been suggested to provide functional coupling of disparate cortical and subcortical regions involved in both error and feedback processing (Luu et al., 2003).

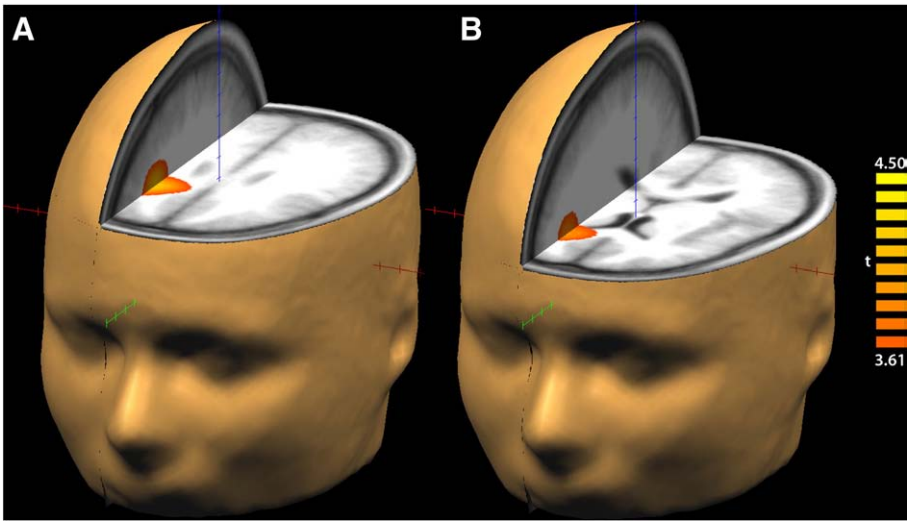

Fig. 5. Cortical generators of theta activity as revealed by beamforming and thresholded at $p<0.001$ (uncorrected for multiple comparisons), (A) after High-Risk Wins and (B) after High-Risk Losses.

Such coupling is probably necessary to support the several sub-processes of reward processing such as discrimination of feedback stimuli and updating any ongoing registration of the probabilities of various outcomes. This notion is consistent with the suggestion that theta-band signals are critical for coordinating activity across large-scale networks (Buzsaki and Draguhn, 2004; Von Stein and Sarnthein, 2000). Furthermore, theta-band activity is believed to be critical during memory processes, for example during encoding stimuli into implicit memory (Klimesch et al., 1996) and during recognition tasks (Doppelmayr et al., 2000; Klimesch et al., 2000).

Luu et al. (2003) investigated the theta-band component of the evoked FRN (rather than induced theta) by bandpass-filtering ERP data between 4–12 Hz. Using a dipole-fitting approach, this study suggested that feedback-evoked theta components were generated by a pair of midline sources, one possibly in rostral ACC and another in dorsal medial frontal cortex. Their study was unable to image sources of induced activity and was unable to resolve different contributions from the two hemispheres. Our results extend this finding in two ways: First, we were able to image the combined effects of induced and evoked theta. Second, by using bilateral multi-source beamforming, our analysis was sensitive to theta-band signals generated in either hemisphere. Since we found significant voxels in the right hemisphere only, we conclude that feedback-induced theta is substantially right-lateralized, as has been suggested by previous work (Gehring and Willoughby, 2004; Marco-Pallares et al., 2008). It should be noted that our Beamformer images (Fig. 5) are statistical parametric maps indicating regions of consistency across participants, rather than maps of grand-averaged theta activity per se. Individuals exhibited substantial variability in their Q maps, including some engagement of the left frontal lobe. This variability probably accounts for the tendency of dipole-fitting approaches to localize midline or bilaterally symmetric sources as the best fitting models when applied to grand-averaged data.

Our approach to analyzing Beamformer volume maps was conservative because it viewed each voxel independently (necessitating an arbitrarily high t-score threshold) rather than as members of larger clusters of functionally related voxels (as would a dipole-fitting approach). Consequently, regions of increased theta power may have been missed. We nevertheless conclude that our results are consistent either with a single theta signal generator on the medial wall of the right frontal lobe, or a group of generators within medial frontal cortex that are closely associated both functionally and anatomically. However, we do not rule out the possibility of less prominent contributing sources, especially in left frontal cortex. Because regions of increased theta power following wins and losses only partially overlapped, we further speculate that feedback is processed by partially distinct networks, depending on its valence.

The role of risk in feedback-related brain responses

The choice of a higher-risk/higher-reward bet led to significantly increased theta amplitude subsequent to feedback in our time–frequency analysis. Our beamforming analysis also found significantly increased Q values in medial frontal cortex following feedback on high-risk but not low-risk bets. This sensitivity to outcome probability is broadly consistent with previous work (Cohen et al., 2007) and might be due to two independent factors. First, the rewards and punishments on high-risk trials were necessarily of greater magnitude (as incentive to take the higher risk). This may contribute greater saliency to the feedback stimulus. Second, in our study participants were implicitly aware of the contingencies of higher and lower risk bets. Thus they may have entered an attentional set upon initiating high-risk bets that potentiated subsequent brain responses. Cohen et al. (2007) found that decreasing reward probability (as in our high- relative to low-risk conditions) led to greater theta-band power following wins but not following losses. By contrast, we found no such dissociation between risk and valence. It thus remains unclear whether attentional set might potentiate induced theta specifically for feedback stimuli or more generally for any subsequent stimulus.

Our results differ from previous reports in other respects: whereas our study found feedback-induced modulations only in the theta-band, Marco-Pallares et al. (2008) and Cohen et al. (2007) also found an increase in power over frontal scalp within the 20 to 30 Hz band at an approximate latency of 250–400 ms following wins relative to losses — a reward-induced response. We found no such increase in this band. These differences may reflect fundamental differences in how reward type modulates feedback processing. In both previous studies the amount of monetary compensation depended on the participant's performance, whereas our subjects received fixed, non-monetary reward. It may be that this higher-frequency activity is the result of exogenous motivation that enhanced the saliency of wins relative to losses among their participants. Further investigation of these discrepant results may elucidate how motivational states are represented during feedback processing.

Acknowledgments

The authors thank Richard Worsey and Andrew Butcher for assistance with experimental design and Dr. Robert Williams and Dr. Robert Sutherland for helpful discussion. GJC is supported by an NSERC USRA scholarship. This work was supported by the Alberta Gaming Research Institute and NSERC Discovery Grants to MST.

References

Bechara, A., Damasio, A.R., Damasio, H., Anderson, S.W., 1994. Insensitivity to future consequences following damage to human prefrontal cortex. Cognition 50, 7–15.
Bellebaum, C., Daum, I., 2008. Learning-related changes in reward expectancy are reflected in the feedback-related negativity. Eur. J. Neurosci. 27, 1823–1835.
Buzsaki, G., Draguhn, A., 2004. Neuronal oscillations in cortical networks. Science 304 , 1926–1929.
Cavedini, P., Riboldi, G., Keller, R., D'Annucci, A., Bellodi, L., 2002. Frontal lobe dysfunction in pathological gambling patients. Biol. Psychiatry 51, 334–341.
Cohen, M.X., 2007. Individual differences and the neural representations of reward expectation and reward prediction error. Soc. Cogn. Affect Neurosci. 2, 20–30.
Cohen, M.X., Elger, C.E., Ranganath, C., 2007. Reward expectation modulates feedback-related negativity and EEG spectra. Neuroimage 35, 968–978.
Cohen, M.X., Elger, C.E., Fell, J., 2008. Oscillatory activity and phase-amplitude coupling in the human medial frontal cortex during decision making. J. Cogn. Neurosci.
Delgado, M.R., Nystrom, L.E., Fissell, C., Noll, D.C., Fiez, J.A., 2000. Tracking the hemodynamic responses to reward and punishment in the striatum. J. Neurophysiol. 84, 3072–3077.
Donkers, F.C., Nieuwenhuis, S., van Boxtel, G.J., 2005. Mediofrontal negativities in the absence of responding. Brain Res. Cogn. Brain Res. 25, 777–787.
Doppelmayr, M., Klimesch, W., Schwaiger, J., Stadler, W., Rohm, D., 2000. The time locked theta response reflects interindividual differences in human memory performance. Neurosci. Lett. 278, 141–144.
Everitt, B.J., Dickinson, A., Robbins, T.W., 2001. The neuropsychological basis of addictive behaviour. Brain Res. Brain Res. Rev. 36, 129–138.
Gehring, W.J., Willoughby, A.R., 2002. The medial frontal cortex and the rapid processing of monetary gains and losses. Science 295, 2279–2282.
Gehring, W.J., Willoughby, A.R., 2004. Are all medial frontal negativities created equal? Toward a richer empirical basis for theories of action monitoring. In: Ullsperger, M., Falkenstein, M. (Eds.), Errors, Conflicts and the Brain. Current Opinions on Performance Monitoring. Max Planck Institute of Cognitive Neuroscience, Leipzig, pp. 14–20.
Goudriaan, A.E., Oosterlaan, J., de Beurs, E., van den Brink, W., 2005. Decision making in pathological gambling: a comparison between pathological gamblers, alcohol dependents, persons with Tourette syndrome, and normal controls. Brain Res. Cogn. Brain Res. 23, 137–151.
Green, J.J., McDonald, J.J., 2008. Electrical neuroimaging reveals timing of attentional control activity in human brain. PLoS Biol. 6, e81.
Green, J.J., McDonald, J.J. (Eds.), in press. A practical guide to beamformer source reconstruction for EEG. MIT Press, Cambridge, MA.
Green, J.J., Conder, J.A., McDonald, J.J., 2008. Lateralized frontal activity elicited by attention-directing visual and auditory cues. Psychophysiology 45, 579–587.
Gross, J., Kujala, J., Hamalainen, M., Timmermann, L., Schnitzler, A., Salmelin, R., 2001. Dynamic imaging of coherent sources: studying neural interactions in the human brain. Proc. Natl. Acad. Sci. U.S.A. 98, 694–699.
Hewig, J., Trippe, R., Hecht, H., Coles, M.G., Holroyd, C.B., Miltner, W.H., 2006. Decision-making in Blackjack: an electrophysiological analysis. Cereb. Cortex.

Hoechstetter, K., Bornfleth, H., Weckesser, D., Ille, N., Berg, P., Scherg, M., 2004. BESA source coherence: a new method to study cortical oscillatory coupling. Brain Topogr. 16, 233–238.
Holroyd, C.B., Coles, M.G., 2002. The neural basis of human error processing: reinforcement learning, dopamine, and the error-related negativity. Psychol. Rev. 109, 679–709.
Holroyd, C.B., Larsen, J.T., Cohen, J.D., 2004. Context dependence of the event-related brain potential associated with reward and punishment. Psychophysiology 41, 245–253.
Holroyd, C.B., Hajcak, G., Larsen, J.T., 2006. The good, the bad and the neutral: electrophysiological responses to feedback stimuli. Brain Res. 1105, 93–101.
Holroyd, C.B., Pakzad-Vaezi, K.L., Krigolson, O.E., 2008. The feedback correct-related positivity: sensitivity of the event-related brain potential to unexpected positive feedback. Psychophysiology 45, 688–697.
Ille, N., Berg, P., Scherg, M., 2002. Artifact correction of the ongoing EEG using spatial filters based on artifact and brain signal topographies. J. Clin. Neurophysiol. 19, 113–124.
Klimesch, W., Doppelmayr, M., Russegger, H., Pachinger, T., 1996. Theta band power in the human scalp EEG and the encoding of new information. Neuroreport 7, 1235–1240.
Klimesch, W., Doppelmayr, M., Schwaiger, J., Winkler, T., Gruber, W., 2000. Theta oscillations and the ERP old/new effect: independent phenomena? Clin. Neurophysiol. 111, 781–793.
Krigolson, O.E., Pierce, L.J., Holroyd, C.B., Tanaka, J.W., 2008. Learning to become an expert: reinforcement learning and the acquisition of perceptual expertise. J. Cogn. Neurosci.
Liu, X., Powell, D.K., Wang, H., Gold, B.T., Corbly, C.R., Joseph, J.E., 2007. Functional dissociation in frontal and striatal areas for processing of positive and negative reward information. J. Neurosci. 27, 4587–4597.
Luu, P., Tucker, D.M., Derryberry, D., Reed, M., Poulsen, C., 2003. Electrophysiological responses to errors and feedback in the process of action regulation. Psychol. Sci. 14, 47–53.
Marco-Pallares, J., Cucurell, D., Cunillera, T., Garcia, R., Andres-Pueyo, A., Munte, T.F., Rodriguez-Fornells, A., 2008. Human oscillatory activity associated to reward processing in a gambling task. Neuropsychologia 46, 241–248.
McClure, S.M., Berns, G.S., Montague, P.R., 2003. Temporal prediction errors in a passive learning task activate human striatum. Neuron 38, 339–346.
McClure, S.M., York, M.K., Montague, P.R., 2004. The neural substrates of reward processing in humans: the modern role of FMRI. Neuroscientist 10, 260–268.
Miltner, W.H.R., Braun, C.H., Coles, M.G.H., 1997. Event-related brain potentials following incorrect feedback in a time-estimation task: evidence for a "generic" neural system for error detection. J. Cogn. Neurosci. 9, 788–798.
Nieuwenhuis, S., Holroyd, C.B., Mol, N., Coles, M.G., 2004a. Reinforcement-related brain potentials from medial frontal cortex: origins and functional significance. Neurosci. Biobehav. Rev. 28, 441–448.
Nieuwenhuis, S., Yeung, N., Holroyd, C.B., Schurger, A., Cohen, J.D., 2004b. Sensitivity of electrophysiological activity from medial frontal cortex to utilitarian and performance feedback. Cereb. Cortex 14, 741–747.
Nieuwenhuis, S., Slagter, H.A., von Geusau, N.J., Heslenfeld, D.J., Holroyd, C.B., 2005. Knowing good from bad: differential activation of human cortical areas by positive and negative outcomes. Eur. J. Neurosci. 21, 3161–3168.
O'Doherty, J., Dayan, P., Schultz, J., Deichmann, R., Friston, K., Dolan, R.J., 2004. Dissociable roles of ventral and dorsal striatum in instrumental conditioning. Science 304, 452–454.
O'Doherty, J.P., Deichmann, R., Critchley, H.D., Dolan, R.J., 2002. Neural responses during anticipation of a primary taste reward. Neuron 33, 815–826.
Oliveira, F.T., McDonald, J.J., Goodman, D., 2007. Performance monitoring in the anterior cingulate is not all error related: expectancy deviation and the representation of action–outcome associations. J. Cogn. Neurosci. 19, 1994–2004.
Oya, H., Adolphs, R., Kawasaki, H., Bechara, A., Damasio, A., Howard 3rd, M.A., 2005. Electrophysiological correlates of reward prediction error recorded in the human prefrontal cortex. Proc. Natl. Acad. Sci. U.S.A. 102, 8351–8356.
Pagnoni, G., Zink, C.F., Montague, P.R., Berns, G.S., 2002. Activity in human ventral striatum locked to errors of reward prediction. Nat. Neurosci. 5, 97–98.
Schonberg, T., Daw, N.D., Joel, D., O'Doherty, J.P., 2007. Reinforcement learning signals in the human striatum distinguish learners from nonlearners during reward-based decision making. J. Neurosci. 27, 12860–12867.
Schultz, W., 2007. Behavioral dopamine signals. Trends Neurosci. 30, 203–210.
Sutton, R.S., Barto, A.G., 1998. Reinforcement learning: an introduction. IEEE Trans. Neural. Netw. 9, 1054.
Van Veen, B.D., van Drongelen, W., Yuchtman, M., Suzuki, A., 1997. Localization of brain electrical activity via linearly constrained minimum variance spatial filtering. IEEE Trans. Biomed. Eng. 44, 867–880.
Von Stein, A., Sarnthein, J., 2000. Different frequencies for different scales of cortical integration: from local gamma to long range alpha/theta synchronization. Int. J. Psychophysiol. 38, 301–313.
Yacubian, J., Glascher, J., Schroeder, K., Sommer, T., Braus, D.F., Buchel, C., 2006. Dissociable systems for gain- and loss-related value predictions and errors of prediction in the human brain. J. Neurosci. 26, 9530–9537.
Yasuda, A., Sato, A., Miyawaki, K., Kumano, H., Kuboki, T., 2004. Error-related negativity reflects detection of negative reward prediction error. Neuroreport 15, 2561–2565.
Yeung, N., Sanfey, A.G., 2004. Independent coding of reward magnitude and valence in the human brain. J. Neurosci. 24, 6258–6264.
Yeung, N., Holroyd, C.B., Cohen, J.D., 2005. ERP correlates of feedback and reward processing in the presence and absence of response choice. Cereb. Cortex 15, 535–544.